Characterization of Acoustic Liners at High Frequencies in a Laboratory Environment

Alexander N. Carr
NASA Langley Research Center, Hampton, VA

Acoustics Liner Workshop
Hampton, VA
March 20, 2023

Acknowledgments

Special thanks to the Advanced Air Transport Technology Project of the NASA Advanced Air Vehicles Program for funding this work

Portions of this presentation focus on experiments led by Mike Jones and Chelsea Solano with contributions from Larry Becker and Doug Nark

Motivation

- 2020 survey indicates liner characterization up to 5 – 6 kHz may be desired
- Liners traditionally tested $\leq$ 3 kHz in LTF [1]
  - Plenty of experimental studies in literature at plane-wave frequencies [2–9]
  - Impedance models validated in the plane-wave regime
  - Lack of background information regarding high frequency impedance testing [10, 11]
- Difficulties associated with high frequency testing that we expected
  - Achieving sufficient SPL at high frequency
  - Different analysis techniques, higher order modes (HOMs) present
- This talk will review
  - Our current progress in high frequency testing in LTF
  - How we have approached expected difficulties
  - How we plan to approach unexpected difficulties

Background: High Intensity Modal Impedance Tube

High Intensity Modal Impedance Tube (HIMIT)

- No flow
- 2″×2″ rectangular waveguide
- Source generation
  - Two compression drivers (155+ dB)
  - Hartmann generator (170 dB)
- 14″ in length
- 0.25″ reference mic, 0.25″ standoff distance from sample face
- 4 rotating plugs, each with 2 mics (0.125″)
- Two-microphone method (plane wave)
- Modal impedance eduction (higher frequencies)
  - Requires microphone calibration
  - Performed in situ with CSQ3 sample

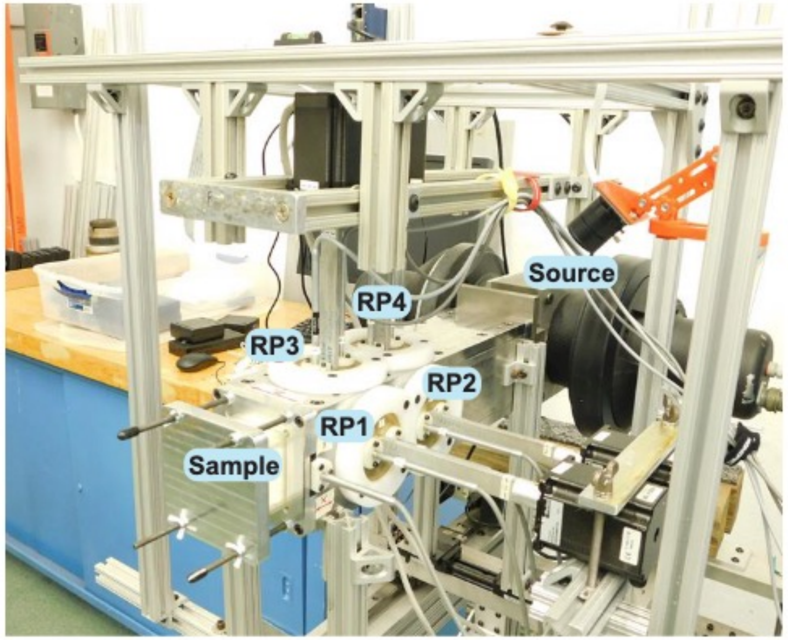

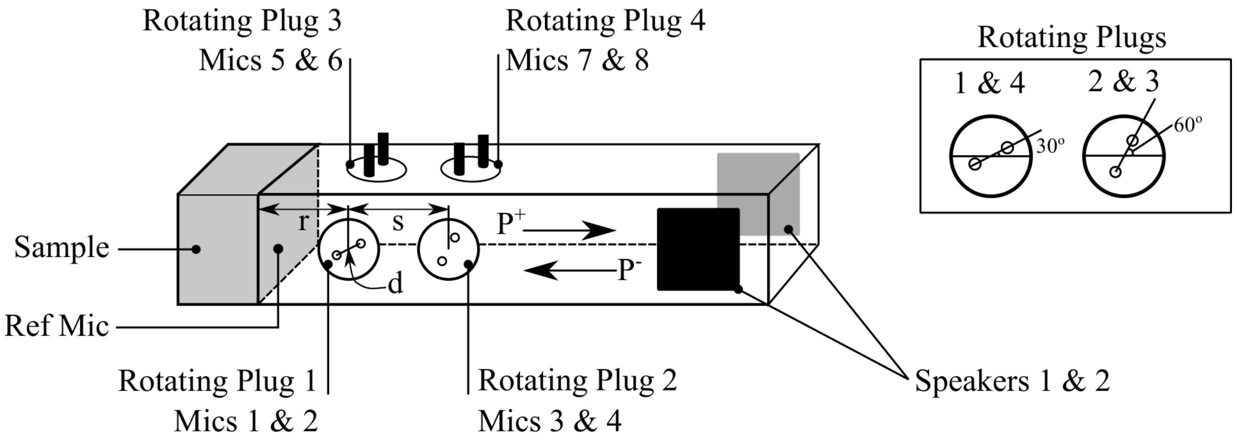

Impedance Eduction with Modal Analysis

Modal Analysis

$$P(x,y,z) = \sum_{n=0}^{\infty}\sum_{m=0}^{\infty}\left[A_{nm}^{+}e^{-i\gamma_{nm}x} + A_{nm}^{-}e^{i\gamma_{nm}x}\right]\Psi_{nm}(y,z)$$

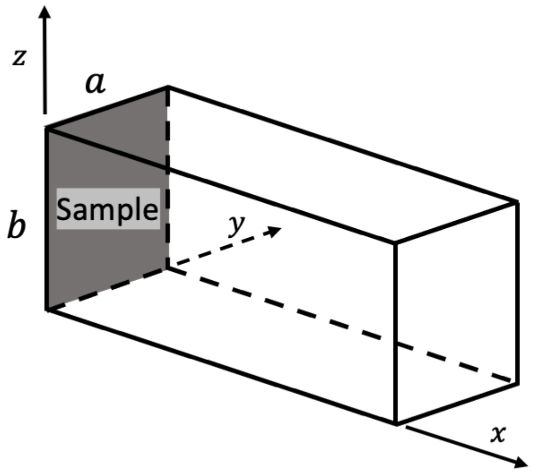

- $\Psi_{\mathrm{nm}}(\mathrm{y},\mathrm{z}) = \cos\left(\frac{\mathrm{n}\pi\mathrm{y}}{\mathrm{a}}\right)\cos\left(\frac{\mathrm{m}\pi\mathrm{z}}{b}\right)$
- 8 mics, take the absolute SPL and phase at each mic
- Solve for the modal amplitudes using the relation: $\boxed{\boldsymbol{A} = [\boldsymbol{T}^{\boldsymbol{T}}\boldsymbol{T}]^{-\boldsymbol{1}}\boldsymbol{T}^{\boldsymbol{T}}\boldsymbol{P}}$

$$\boldsymbol{P} = \begin{bmatrix} P(x_1,y_1,z_1) \\ \vdots \\ P(x_8,y_8,z_8) \end{bmatrix} \quad \boldsymbol{T} = \begin{bmatrix} T_{00}^{+}(x_1,y_1,z_1) & \cdots & T_{NM}^{+}(x_1,y_1,z_1) & T_{00}^{-}(x_1,y_1,z_1) & \cdots & T_{NM}^{-}(x_1,y_1,z_1) \\ \vdots & \ddots & \vdots & \vdots & \ddots & \vdots \\ T_{00}^{+}(x_8,y_8,z_8) & \cdots & T_{NM}^{+}(x_8,y_8,z_8) & T_{00}^{-}(x_8,y_8,z_8) & \cdots & T_{NM}^{-}(x_8,y_8,z_8) \end{bmatrix} \quad \boldsymbol{A} = \begin{bmatrix} A_{00}^{+} \\ \vdots \\ A_{NM}^{+} \\ A_{00}^{-} \\ \vdots \\ A_{NM}^{-} \end{bmatrix}$$

- $T_{nm}^{+}(x_i,y_i,z_i) = e^{-i\gamma_{nm}x_i}\Psi_{\mathrm{nm}}(y_i,z_i)$ and $T_{nm}^{-}(x_i,y_i,z_i) = e^{i\gamma_{nm}x_i}\Psi_{\mathrm{nm}}(y_i,z_i)$
- $[\boldsymbol{T}^{\boldsymbol{T}}\boldsymbol{T}]^{-\boldsymbol{1}}\boldsymbol{T}^{\boldsymbol{T}}$ is computed using singular value decomposition
- Method is **most accurate** for predicting the **dominant mode**

Impedance Eduction with Modal Analysis

Impedance Eduction

- Normalized specific acoustic impedance of the sample

$$\zeta = -\frac{P}{\rho c U_x} = -k\frac{\sum_{n=0}^{\infty}\sum_{m=0}^{\infty}\left[A_{nm}^{+}e^{-ik_x x} + A_{nm}^{-}e^{ik_x x}\right]\Psi_{nm}(y,z)}{\sum_{n=0}^{\infty}\sum_{m=0}^{\infty}\gamma_{nm}\left[A_{nm}^{+}e^{-ik_x x} - A_{nm}^{-}e^{ik_x x}\right]\Psi_{nm}(y,z)}$$

- Impedance for a single mode

$$\boxed{\zeta_{nm,nm} = \frac{k}{\gamma_{nm}}\frac{1 + R_{nm,nm}}{1 - R_{nm,nm}}} \qquad (1)$$

- $R_{nm,nm} = A_{nm}^{+}/A_{nm}^{-}$
- Accurate for the dominant mode with large separation from other modes
- Impedance should be computed for mode with highest power

Investigations with HIMIT (so far)

HIMIT Checkout (Jones et al. [12])

- Two samples: CSQ3 and GE01
- Frequencies up to 6 kHz (CSQ3)
- SPL up to 155 dB (GE01)

Results

- Agreement between impedance of modes with highest power and ZKTL
- Increase in θ of GE01 with SPL

CSQ3

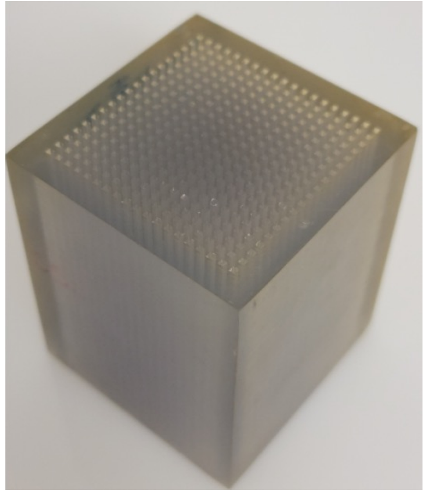

GE01

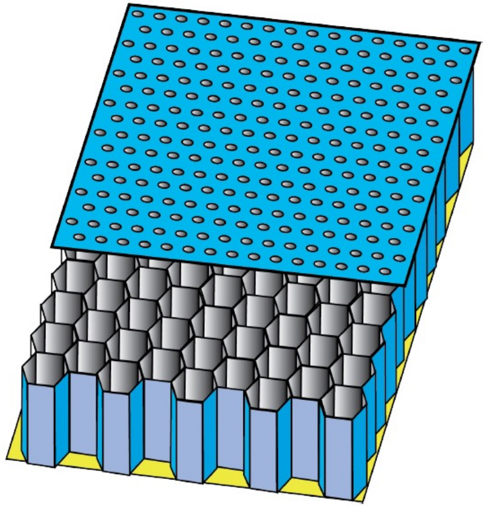

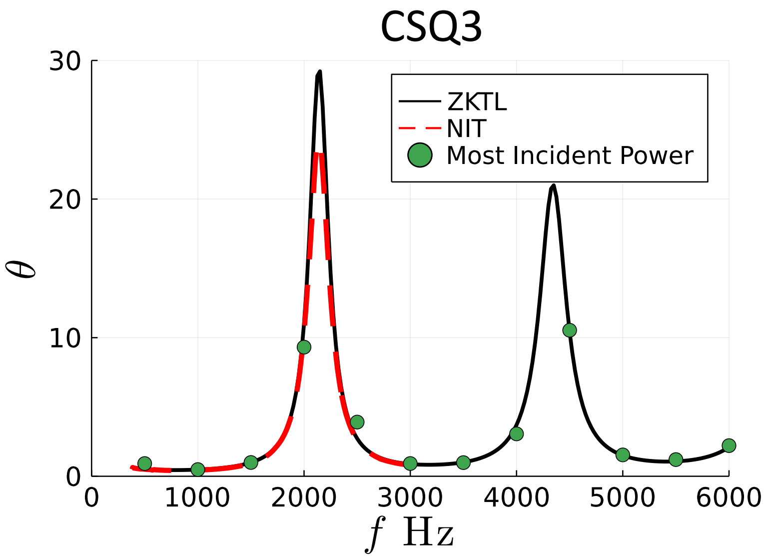

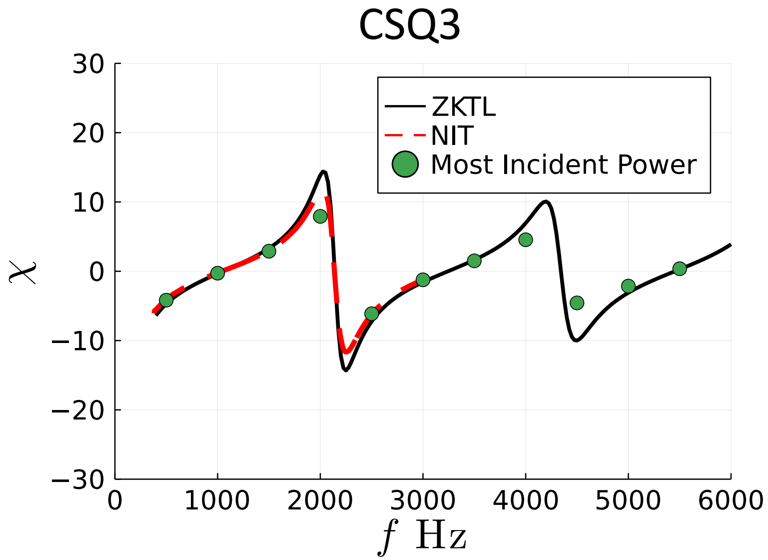

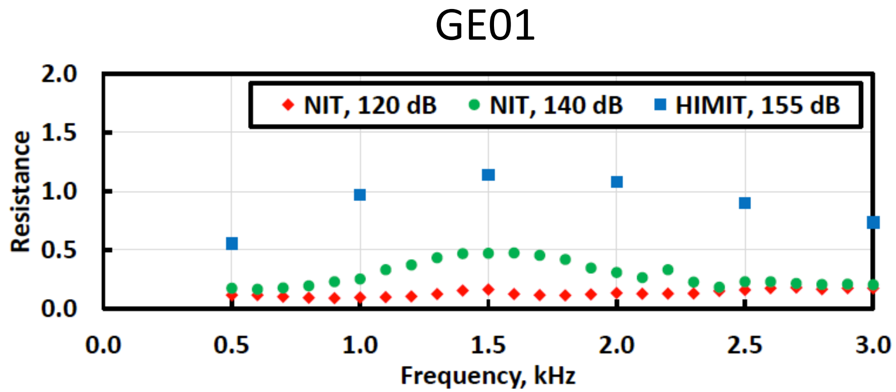

Investigations with HIMIT (so far)

Follow on Study (Solano et al. [13])

- C15R27: mesh over honeycomb
- A015 and A024: over the rotor samples
- 120 dB, 140 dB, and 150 dB
- $0.4 \leq f \leq 6.0$ kHz (150 dB; $f \leq 3.0$ kHz)

Results

- GE01 and A015
  - Highest power mode provides consistent results

C15R27

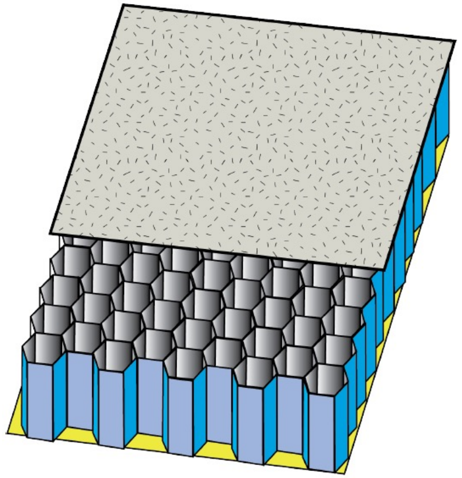

A015

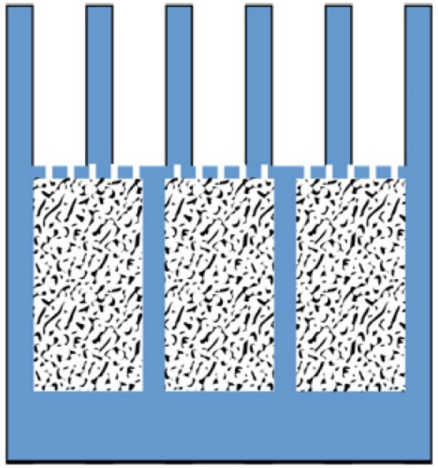

GE01

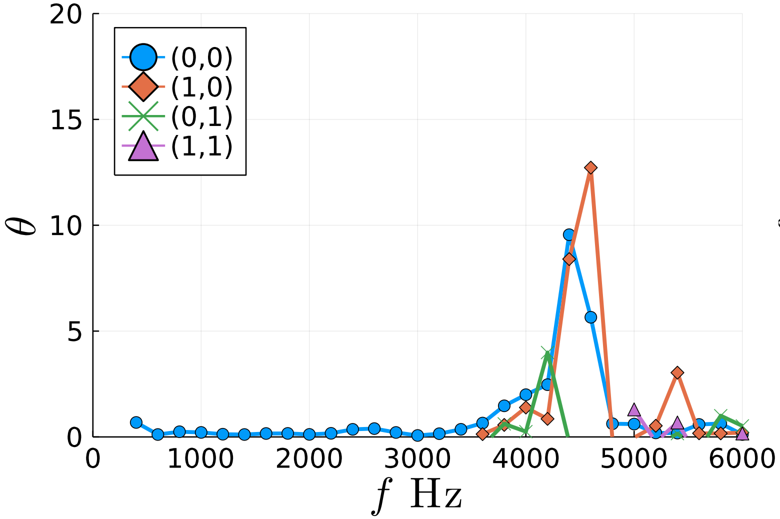

GE01

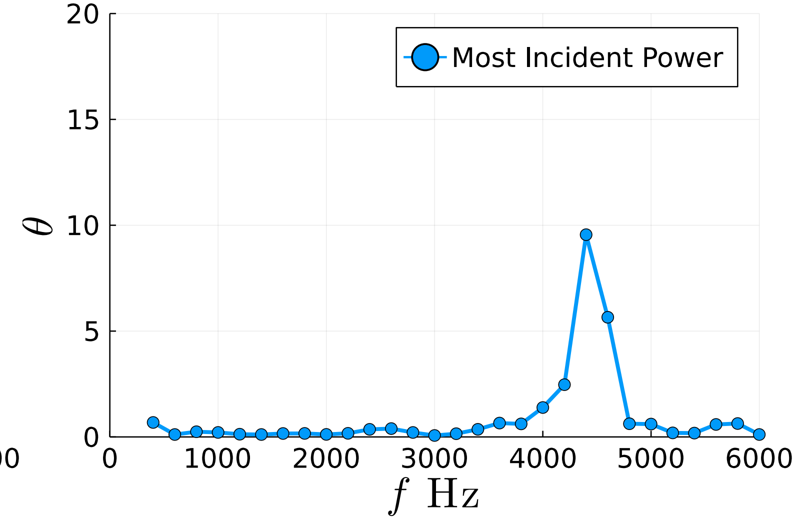

A024

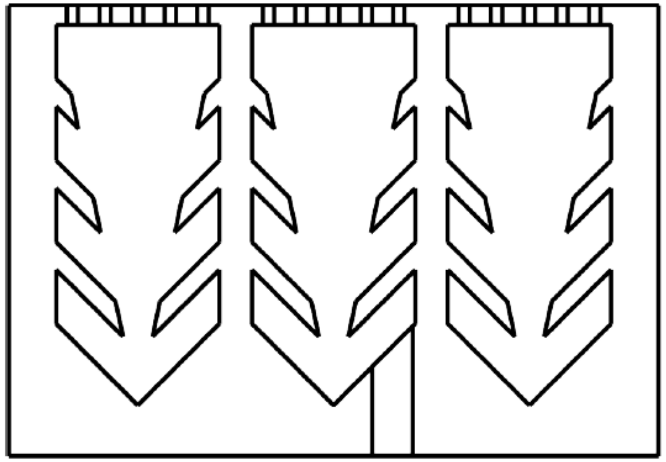

Current Issues: A024 Sample

Follow on Study (Solano et al. [13])

- A024 Results
  - Inconsistencies when using the highest power mode
  - Negative resistance values – nonphysical
  - Choosing mode with highest SPL does not help
  - COMSOL modeling?

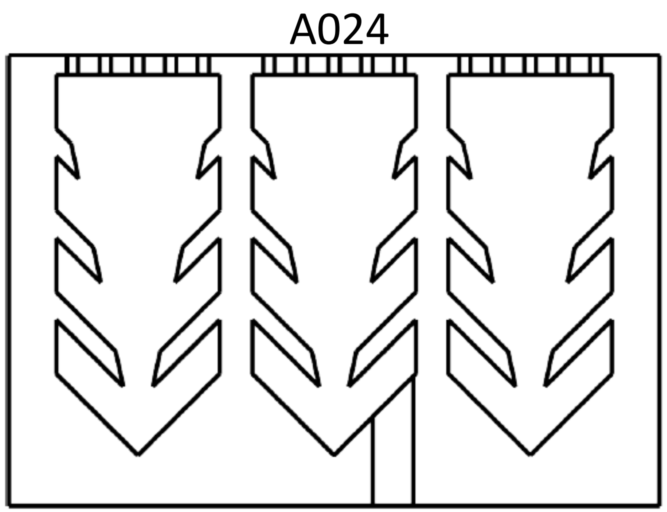

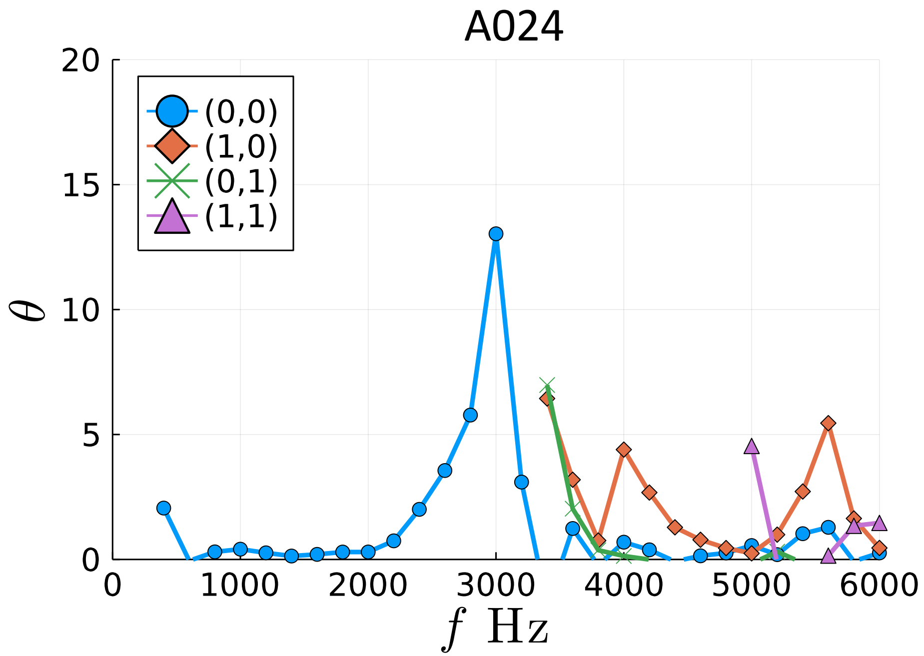

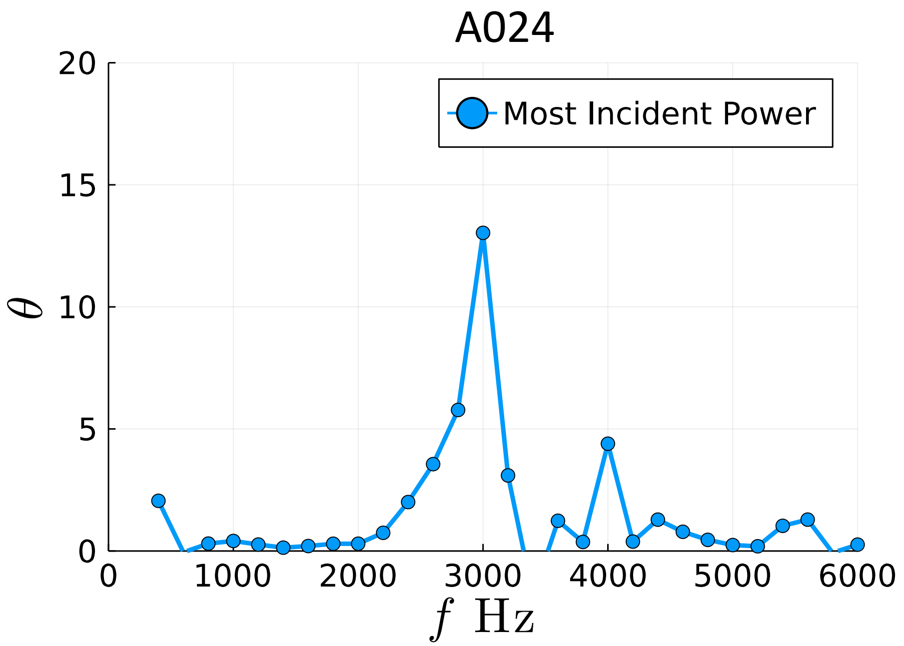

Current Issues: Mode Control

- Multiple modes contribute significantly around 4 kHz
- Modal decomposition approach works best when 1 mode is dominant
- Desire to have mode control (similar to CDTR) to avoid this issue
- Schultz et al. [10] – able to achieve 20 dB separation with blocker plate

(1,1) blocker plate

CSQ3

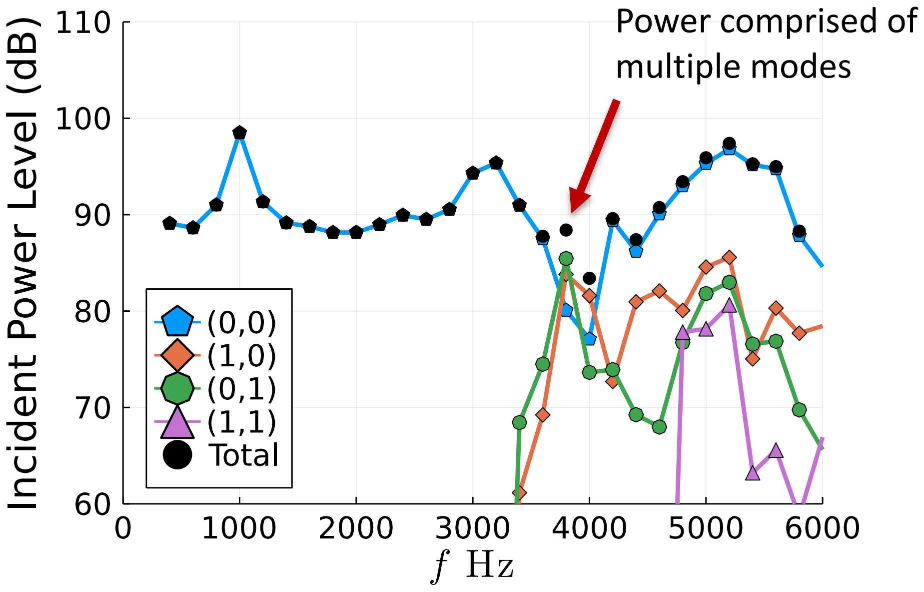

A024

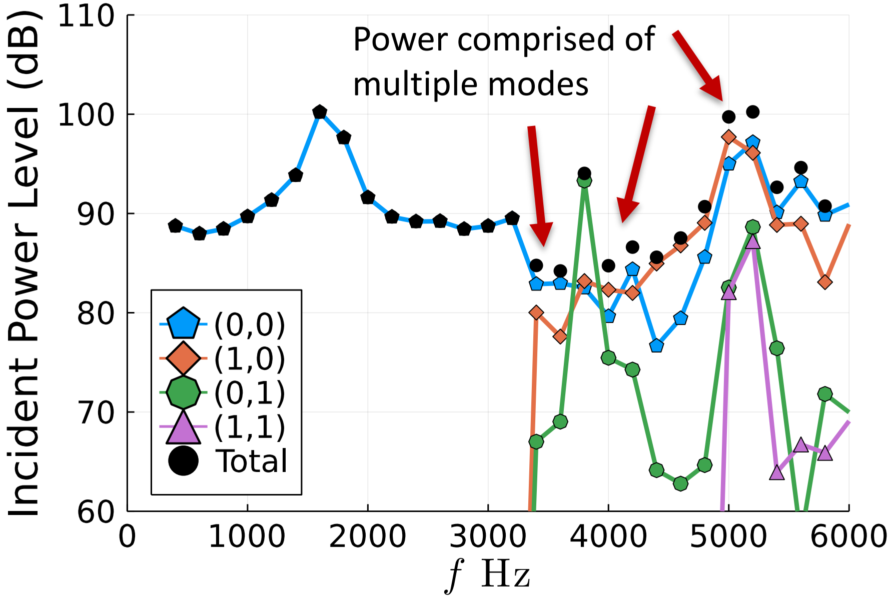

Current Issues: Level Setting in HIMIT

Reference microphone location

- Not ideal for HOMs
- $\frac{1}{4}$ inch microphone, as opposed to $\frac{1}{8}$ inch plug mics
- Measuring SPL $\frac{1}{4}$ inch away from sample

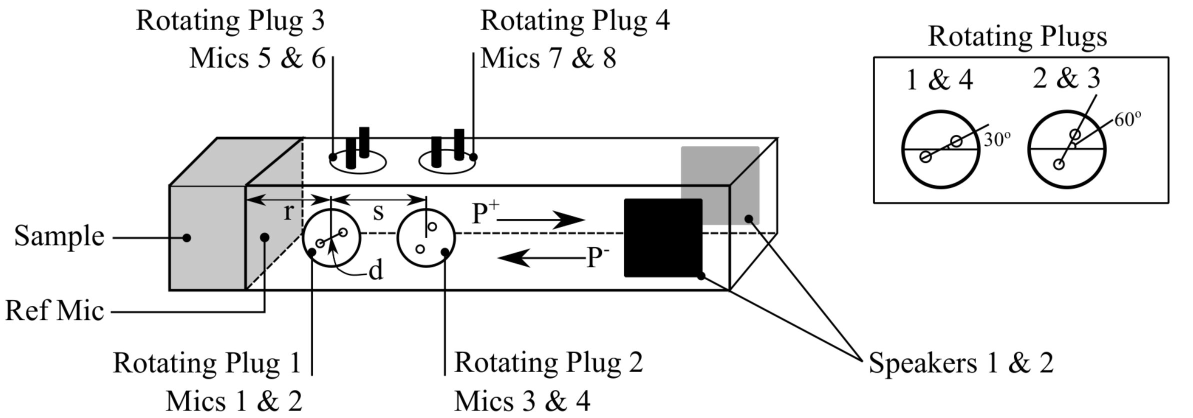

Modal Decomposition Method to set level

- May alleviate some of these difficulties
- 8 microphones to set the level
  - Use modal amplitudes to approximate SPL at face of sample
  - Insensitive to null locations with proper microphone placement
- Level setting options
  - Total, incident, or reflected **mode** power
  - Total, incident, or reflected **mode** SPL
  - **Average** total, incident, or reflected SPL at the sample face
- Implications for nonlinear samples? (perforate over honeycomb)

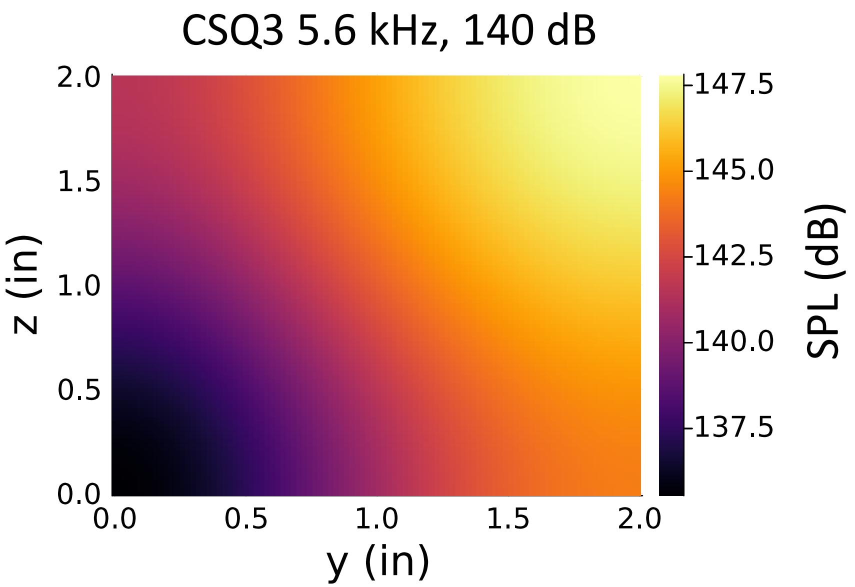

Grazing Flow Impedance Tube (GFIT)

High Frequency Testing in GFIT

- We intend to go up to 6 kHz in GFIT by the end of the year
- Modal decomposition upstream and downstream
  - Need to utilize all mics in those arrays
- Likely need mode control in GFIT as well
- Impedance eduction [14]
  - Objective function method – CHE simulations in 3D
  - Prony – can handle vertical modes
  - Any desire for 3D shear flow with horizontal modes?
- In the meantime, examine mode attenuation

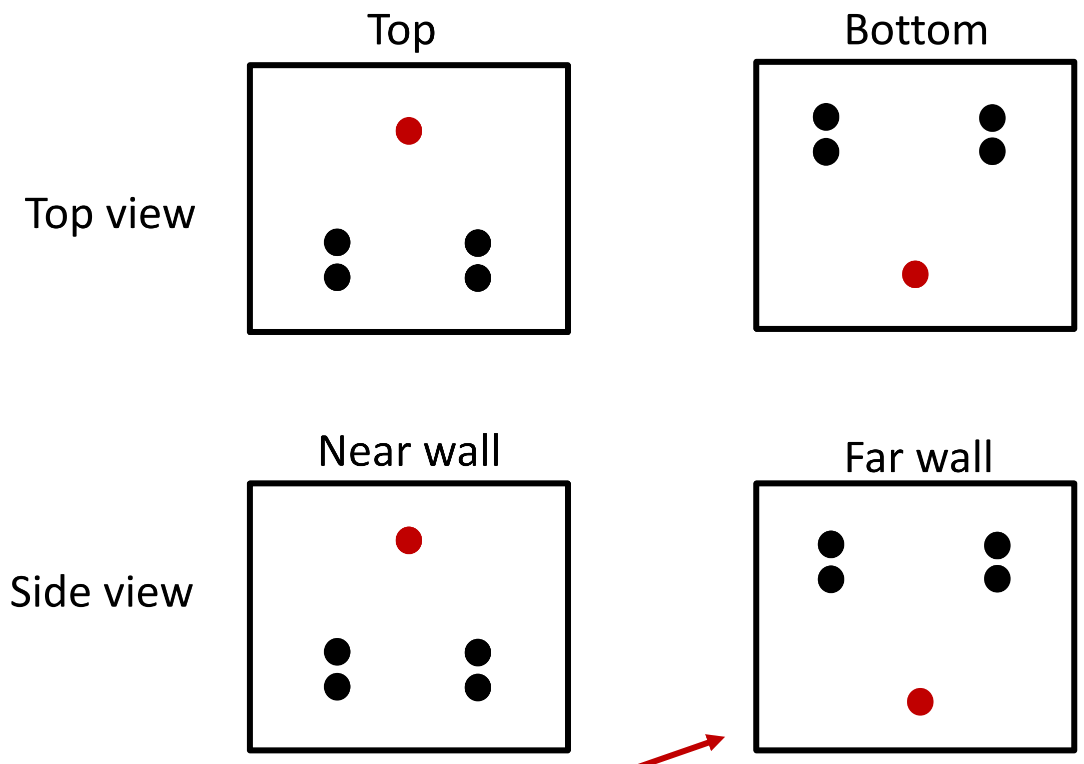

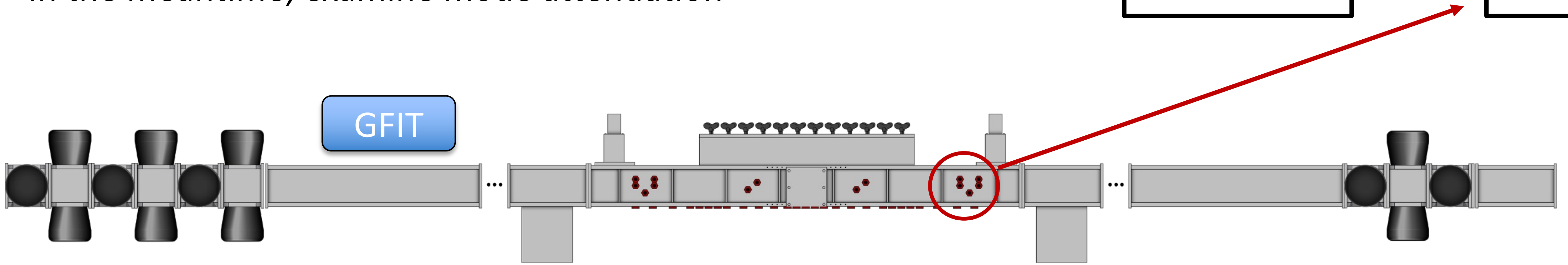

Summary and Future Work

Summary

- Multiple samples have been tested in HIMIT up to 6 kHz and up to 155 dB
- Impedance educed from mode with most incident power
- Our current analysis techniques work best when a single mode is dominant
    - Engine environments have many modes present
- Current obstacles
    - Setting level at sample face – SPL varies along cross-section

Future Work

- Set level with modal decomposition method
- Mode control
- Investigate educed impedance of HOMs at high amplitudes
- Implement modal decomposition in GFIT upstream and downstream arrays
    - Intend to go up to 6 kHz by the end of the year

Questions?

References

[1] M. G. Jones, W. R. Watson, D. M. Nark, B. M. Howerton, and M. C. Brown, “A Review of Acoustic Liner Experimental Characterization at NASA Langley,” 2020, doi: 10.13140/RG.2.2.15613.10720.

[2] X. Jing, S. Peng, and X. Sun, “A straightforward method for wall impedance eduction in a flow duct,” *The Journal of the Acoustical Society of America*, vol. 124, no. 1, pp. 227–234, Jul. 2008, doi: 10.1121/1.2932256.

[3] A. F. Seybert and D. F. Ross, “Experimental determination of acoustic properties using a two-microphone random-excitation technique,” *The Journal of the Acoustical Society of America*, vol. 61, no. 5, 1977.

[4] Y. Renou and Y. Aurégan, “Failure of the Ingard–Myers boundary condition for a lined duct: An experimental investigation,” *The Journal of the Acoustical Society of America*, vol. 130, no. 1, pp. 52–60, Jul. 2011, doi: 10.1121/1.3586789.

[5] A. S. Hersh, B. E. Walker, and J. W. Celano, “Helmholtz Resonator Impedance Model, Part 1: Nonlinear Behavior,” *AIAA Journal*, vol. 41, no. 5, pp. 795–808, May 2003, doi: 10.2514/2.2041.

[6] S.-H. Jang and J.-G. Ih, “On the multiple microphone method for measuring in-duct acoustic properties in the presence of mean flow,” *The Journal of the Acoustical Society of America*, vol. 103, no. 3, pp. 1520–1526, Mar. 1998, doi: 10.1121/1.421289.

[7] X. Jing and X. Sun, “Sound-excited flow and acoustic nonlinearity at an orifice,” *Physics of Fluids*, vol. 14, no. 1, pp. 268–276, Jan. 2002, doi: 10.1063/1.1423934.

[8] T. H. Melling, “The acoustic impendance of perforates at medium and high sound pressure levels,” *Journal of Sound and Vibration*, vol. 29, no. 1, pp. 1–65, Jul. 1973, doi: 10.1016/S0022-460X(73)80125-7.

References

[9] J. Y. Chung and D. A. Blaser, “Transfer function method of measuring in-duct acoustic properties. I. Theory,” *The Journal of the Acoustical Society of America*, vol. 68, no. 3, pp. 907–913, Sep. 1980, doi: 10.1121/1.384778.

[10] T. Schultz, L. N. Cattafesta, and M. Sheplak, “Modal decomposition method for acoustic impedance testing in square ducts,” *The Journal of the Acoustical Society of America*, vol. 120, no. 6, pp. 3750–3758, Dec. 2006, doi: 10.1121/1.2360423.

[11] R. Boucheron, “Modal decomposition method in rectangular ducts in a test-section of a cavitation tunnel with a simultaneous estimate of the effective wall impedance,” *Ocean Engineering*, vol. 209, p. 107491, Aug. 2020, doi: 10.1016/j.oceaneng.2020.107491.

[12] M. G. Jones, A. N. Carr, D. M. Nark, and L. E. Becker, “Implementation of the NASA High Intensity Modal Impedance Tube”.

[13] C. Solano, M. G. Jones, A. N. Carr, and D. M. Nark, “High Intensity Modal Impedance Tube Development at NASA Langley”.

[14] W. R. Watson, M. H. Carpenter, and M. G. Jones, “Performance of Kumaresan and Tufts Algorithm in Liner Impedance Eduction with Flow,” *AIAA Journal*, vol. 53, no. 4, pp. 1091–1102, Apr. 2015, doi: 10.2514/1.J053705.

[15] Hubbard, Harvey H., ed.: Aeroacoustics of Flight Vehicles: Theory and Practice. Volume 2: Noise Control. NASA RP–1258–VOL–2, 1991.

[16] I. B. Crandall 1927 Theory of Vibrating Systems and Sound. New York: D. Van Nostrand & Co. Inc.

Backup Slides

Background: NASA LaRC Liner Technology Facility

High Intensity Modal Impedance Tube (HIMIT)

- Mach 0.0, SPL ≤ 170 dB, Freq ≤ **6 kHz**
- Tone and Broadband sources

Normal Incidence Tube (NIT)

- Mach 0.0, SPL ≤ 155 dB, Freq ≤ 3 kHz
- Tone and Broadband sources

Grazing Flow Impedance Tube (GFIT)

- Mach ≤ 0.6, SPL ≤ 155 dB, Freq ≤ **3 kHz**
- Tone source

Curved Duct Test Rig (CDTR)

- Mach ≤ 0.5, SPL ≤ 135 dB, Freq ≤ 3 kHz
- *Controlled* Tonal mode and Broadband sources

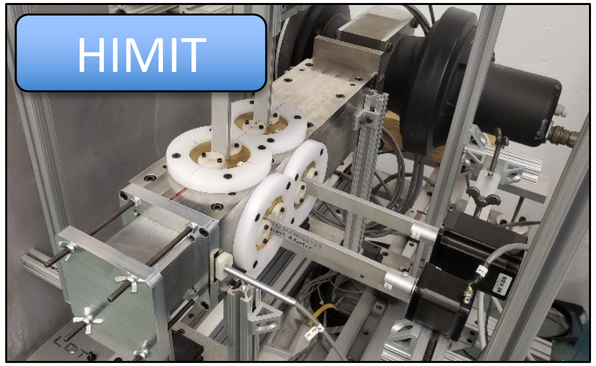

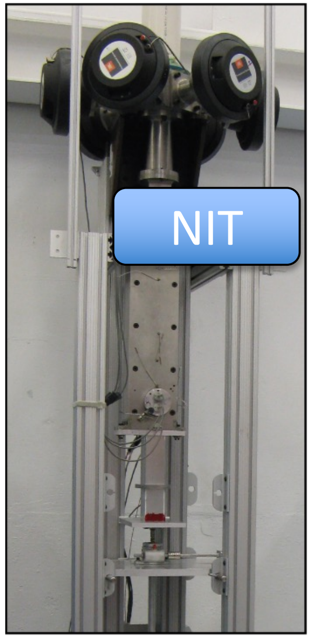

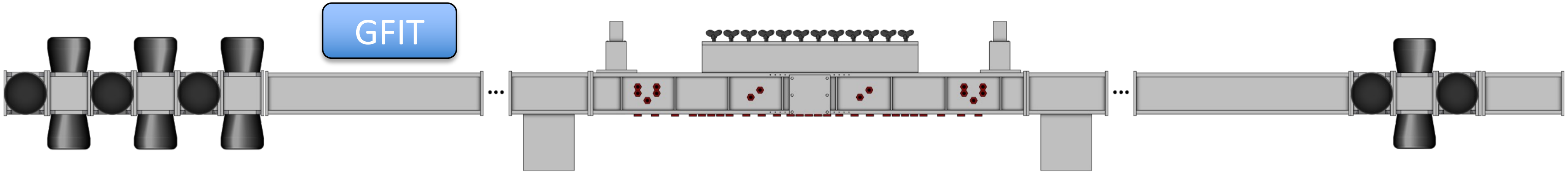

Current Issues: Impedance of Higher Order Modes

Perforate over Honeycomb

- Resistance proportional to rms acoustic velocity at high SPL
- Two parameter, Motsinger and Kraft [15], Crandall [16]

$$\theta_i = A + BV_i$$

$$u_{rms}^{(i)} = \frac{\left|U_x^{(i)}\right|}{\sqrt{2}}$$

- Sample face will be exposed to varying SPL when HOMs dominate
- Resistance may need to be computed as an average over all the holes

$$\theta_{eff} = \frac{1}{N_h}\sum_{i=1}^{N_h}\theta_i = A + \frac{B}{N_h}\sum_{i=1}^{N_h}\frac{\left|U_x^{(i)}\right|}{\sqrt{2}}$$

- Replace the summation with an integral

$$\frac{1}{N_h}\sum_{i=1}^{N_h}\frac{\left|U_x^{(i)}\right|}{\sqrt{2}} \approx \frac{1}{ab}\int_0^b\int_0^a\frac{\left|U_x^{(i)}\right|}{\sqrt{2}}\,dy\,dz$$

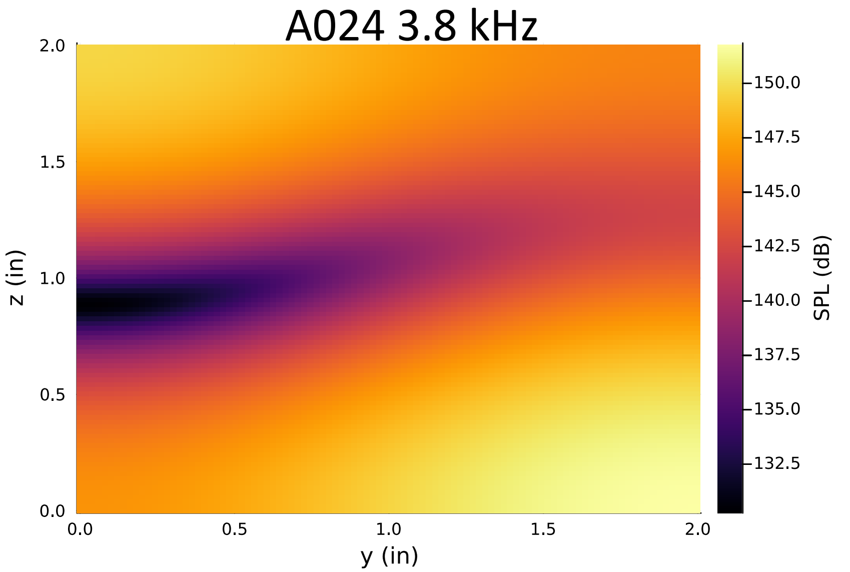

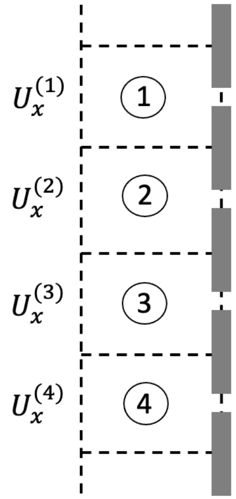

Preliminary Modification to Liner Models

- Eqn. 1 obtained with linear momentum relation

$$i\rho c k U_x = -\frac{\partial P}{\partial x}$$

- This breaks down near surface of liner
- Resort to liner models to understand what may happen when a HOM is dominant
- Two parameter, Mot and Kraft, Crandall

$$\theta_i = A + BV_i$$

- V_i may be replaced by acoustic rms velocity

$$u_{rms}^{(i)} = \frac{\left|U_x^{(i)}\right|}{\sqrt{2}}$$

- The "effective" resistance of the liner may be the average of all the holes

$$\theta_{eff} = \frac{1}{N_h}\sum_{i=1}^{N_h}\theta_i = A + \frac{B}{N_h}\sum_{i=1}^{N_h}\frac{\left|U_x^{(i)}\right|}{\sqrt{2}}$$

- Replace the summation with an integral

$$\frac{1}{N_h}\sum_{i=1}^{N_h}\frac{\left|U_x^{(i)}\right|}{\sqrt{2}} \approx \frac{1}{ab}\int_0^b\int_0^a\frac{\left|U_x^{(i)}\right|}{\sqrt{2}}\,dy\,dz$$

Preliminary Modification to Liner Models

- Consider the case where only one mode is dominant
- If this is the plane-wave mode, then

$$\theta_{eff}^{00} = A + \frac{B}{\rho c}\frac{|R_{00}-1|}{\sqrt{2}}|A_{00}^{-}|$$

- The resistance for any HOM is

$$\theta_{eff}^{nm} = A + \frac{B}{\rho c}\frac{|\gamma_{nm}|}{k}\left(\frac{\sqrt{2}}{\pi}\right)^{\alpha_{nm}}|R_{nm}-1||A_{nm}^{-}|$$

- Where the following relations were used

$$\frac{1}{ab}\int_0^b\int_0^a \frac{|\Psi_{01}|}{\sqrt{2}}dy\,dz = \frac{1}{ab}\int_0^b\int_0^a \frac{|\Psi_{10}|}{\sqrt{2}}dy\,dz = \frac{\sqrt{2}}{\pi} \qquad \frac{1}{ab}\int_0^b\int_0^a \frac{|\Psi_{11}|}{\sqrt{2}}dy\,dz = \left(\frac{\sqrt{2}}{\pi}\right)^2$$

- Ratio of resistance of HOM to plane-wave mode

$$\frac{\theta_{eff}^{nm}-A}{\theta_{eff}^{00}-A} = \frac{|\gamma_{nm}|}{k}\left(\frac{2}{\pi}\right)^{\alpha_{nm}}\frac{|R_{nm}-1|}{|R_{00}-1|}\frac{|A_{nm}^{-}|}{|A_{00}^{-}|} \qquad (2)$$

- It’s possible that “effective” resistance is being measured when Eqn. 1 is used

Preliminary Modification to Liner Models

- Bounds

$$\frac{|\gamma_{nm}|}{k} \leq 1 \qquad \left(\frac{2}{\pi}\right)^{\alpha_{nm}} \leq 1$$

- Implies that

$$\frac{\theta_{eff}^{nm} - A}{\theta_{eff}^{00} - A} \leq \frac{|R_{nm} - 1|}{|R_{00} - 1|} \frac{|A_{nm}^{-}|}{|A_{00}^{-}|}$$

- For the same incident level, will reflection coefficient adjust to keep resistance constant across different modes?